Aircraft System Noise Assessment of the NASA Single-Aisle Over-the-Wing Nacelle Configuration

Kelly M. Shelts[1], Ian A. Clark[2], Russell H. Thomas[3], and Yueping Guo[4]
NASA Langley Research Center, Hampton, VA 23681 USA

A system noise assessment of the NASA single-aisle over-wing nacelle configuration, the OWN160, is carried out to estimate the performance of the configuration relative to NASA noise goals. The vehicle was first designed during the Environmentally Responsible Aviation (ERA) project, and last analyzed in 2016. Renewed interest in the concept necessitates an updated acoustic prediction. A model for jet-trailing-edge interaction noise is developed from experimental data and included in the system noise assessment and analysis. Total system noise is predicted using NASA's research-level Aircraft Noise Prediction Program (ANOPP-Research). Results are evaluated with and without the jet-trailing-edge effect and compared to prior analysis and an equivalent conventional aircraft configuration, the TW160. The jet-trailing-edge interaction affects the noise source ranking and increases the total noise of the OWN160, but the concept retains an advantage for noise reduction when compared to the conventional configuration with a cumulative reduction of 7.7 EPNdB (ERA results showed a 9.7 EPNdB reduction).

I. Introduction

Within the Advanced Air Vehicles Program (AAVP) of the Aeronautics Research Mission Directorate, the NASA Advanced Air Transport Technology Project (AATT) explores and develops technologies and concepts for improved energy efficiency and environmental compatibility for fixed-wing, subsonic transport vehicles. In the midterm timeframe (i.e., between 2025 and 2035), AATT has several goals. First, AATT aims to reduce noise to a 25-35 EPNdB (estimated perceived noise level in decibels) cumulative margin below the Federal Aviation Administration (FAA) Stage 5 certification requirement. The second goal is to reduce landing and takeoff NOx (oxides of nitrogen) emission by 80% relative to CAEP6 (Committee on Environmental Protection) standards and cruise NOx by 80% relative to a 2005 best in class vehicle. Third, AATT aims to reduce fuel consumption by 50-60% relative to a 2005 best in class vehicle [1]. To achieve these goals, AATT must develop concepts and technologies to a technology readiness level of 5-6 within the allotted time frame. Conventional tube-and-wing aircraft configurations cannot likely meet the noise goals [2], which necessitates different airframe configuration concepts.

One concept being considered is an over-wing-nacelle (OWN) aircraft configuration – a tube-and-wing style aircraft with engines mounted above the wings, rather than below. This unconventional aircraft design has potential benefits for noise, aerodynamic performance, and fuel efficiency. While the idea of mounting an engine above a wing is not new, as many military and smaller aircraft incorporate this feature, it was not considered feasible for commercial subsonic vehicles until researchers optimized the design in the 1990s [3-4]. There are several advantages of an over-wing configuration, such as additional taxi and runway clearance (e.g., less likelihood of foreign object debris ingestion) and lower community noise. Kinney and Hahn received a patent for a wing design to support an OWN in 2011, as shown in Fig. 1 [5]. Their design included several important features, such as an inboard wing section with small or no leading edge sweep, a "slipper" turbofan engine integration into the wing that did not include a pylon, and improved aerodynamic design to confine a shock over the leading edge of the wing. This design became the basis for future NASA OWN aircraft concepts.

---

[1] Research Aerospace Engineer, Aeroacoustics Branch, MS 461, kelly.m.shelts@nasa.gov, AIAA Member
[2] Research Aerospace Engineer, Aeroacoustics Branch, MS 461, AIAA Member
[3,4] Senior Research Engineer, Aeroacoustics Branch, MS 461, AIAA Associate Fellow

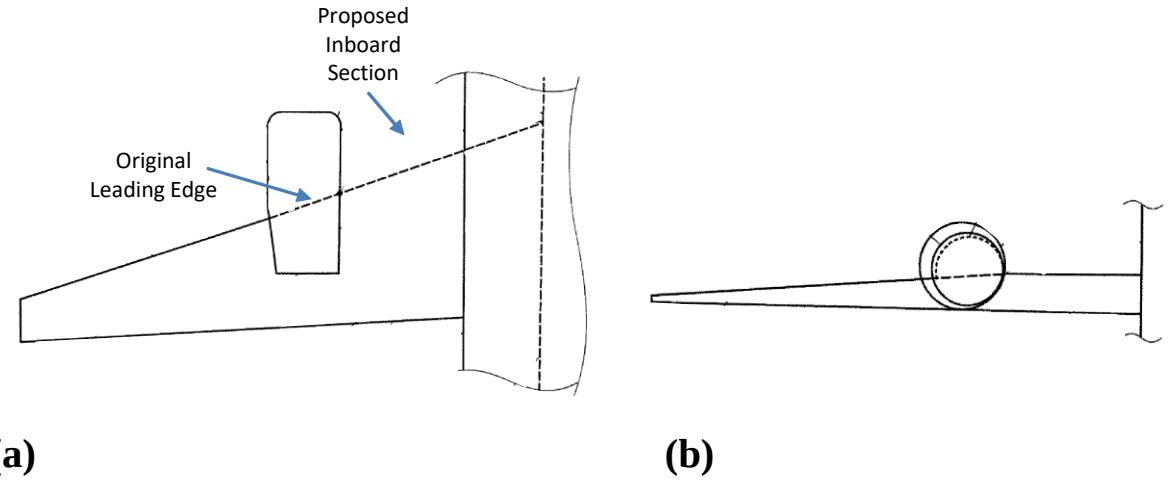

Fig. 1 Aircraft Wing for Over-the-Wing Mounting of Engine Nacelle [5] **(a) top view and (b) front view.**

Later in the 2010s, the Environmentally Responsible Aviation (ERA) project developed several aircraft configuration concepts to simultaneously meet noise, emissions, and fuel burn goals [6]. During this process, ERA took the OWN concept and developed it further for the midterm timeframe. The resulting model was the OWN160, a single-aisle subsonic commercial transport designed for 160 passengers. The TW160, an equivalent, conventional-styled tube-and-wing aircraft, was also designed using the same optimization process. The two vehicles have very different designs, as shown in Fig. 2, and are treated as peers since they were designed for the same passenger class and mission.

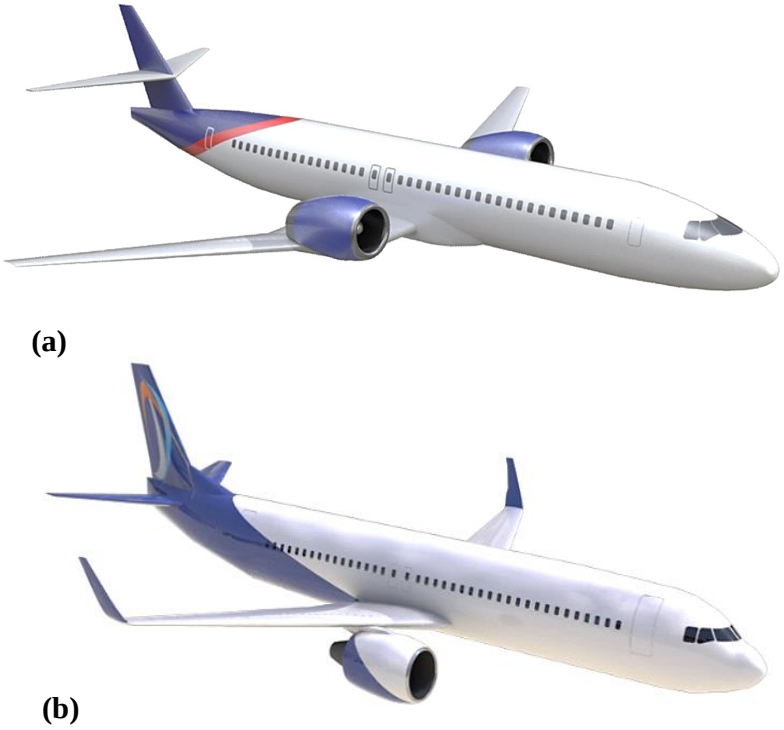

Fig. 2 Artist renderings of the NASA ERA (a) OWN160 and (b) TW160 subsonic transport concepts.

The OWN160 performed favorably in terms of noise reduction when compared to other vehicle models from the ERA project, as shown in Fig. 3. The vehicle configurations considered are shown against their cumulative noise levels below the Stage 4 FAA requirement [2]. The results for the N+2 timeframe are shown in solid bars and results including three additional Integrated Technology Demonstrators for Noise Reduction (ITDNR) technologies are shown in patterned bars. The three noise reduction technologies were: soft vane acoustic treatment applied to the propulsor stator vane, partial main gear fairing, and an acoustic treatment applied to the flap side edge. All three were included, as they were deemed to be maturable in the allotted timeframe. The OWN160 was the second quietest vehicle considered among all configurations and size classes. During ERA, the focus was on larger twin-aisle vehicles due to industry trends, so the OWN160 concept was not pursued further. Since then, NASA has shifted focus to smaller single-aisle vehicles, and an OWN vehicle is an attractive revolutionary aircraft concept, which has motivated the in-depth analysis reported in this paper.

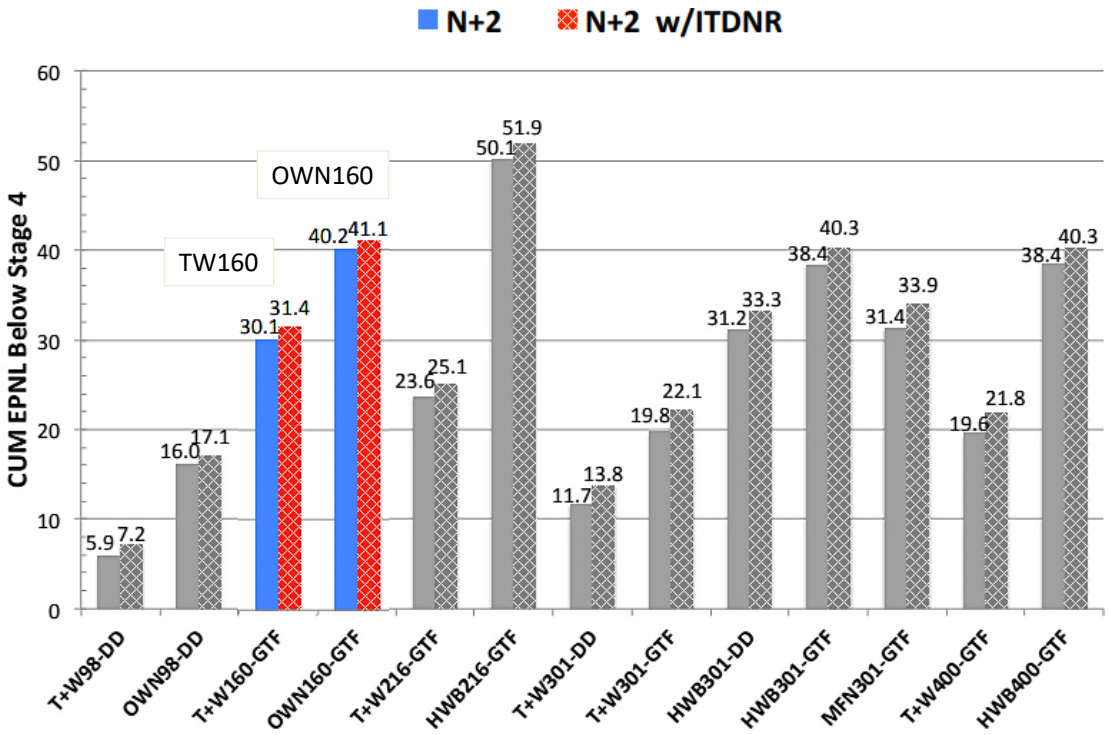

Fig. 3 Aircraft system level noise for all ERA N+2 vehicles, relative to FAA Stage 4 noise requirement [2].

An OWN vehicle has many potential acoustic advantages. If an engine is placed above the wing at the leading edge, the wing will shield ground observers from the aft radiated engine noise. This placement can also incorporate larger diameter engines with higher bypass ratios, which have lower fan pressure ratios, resulting in reduced fan noise emission. Engine placement above the wing also reduces ground clearance concerns, allowing for the use of shorter landing gear, which reduces noise on approach by moving the sources closer to the wing where the mean flow velocity is lower. Another possible advantage is a faster climb out from an upper surface blowing lift advantage. As the jet exhaust flows over the top of the wing, it stays attached to the upper surface longer than for a conventional configuration, creating additional lift [7].

The first objective of this study is to update the system noise prediction for the OWN160, with noise modeling improvements that have been developed since the ERA study. Second, a noise model for a jet-trailing-edge (Jet-TE) interaction source is presented and included in the updated OWN160 prediction to assess system level impacts. Third, the updated OWN160 predictions are compared with the equivalently updated TW160 prediction, as well as the previous ERA noise prediction.

II. Aircraft Configurations

The OWN160 and TW160 were designed using the process described in Ref. [6] for the ERA midterm timeframe and include technology assumptions appropriate for that timeline. The NASA Flight Optimization System (FLOPS) [8] was used to create full vehicle models with proper sizing of aircraft components. The NASA Numerical Propulsion Simulation System (NPSS) [9] was used to design the thermodynamic engine cycle for each aircraft. The NASA Weight Analysis of Gas Turbine Engines (WATE++) [10] was used to create engine component architecture given an engine cycle from NPSS. Basic aircraft parameters for the final designs are shown in Table 1.

Table 1 Parameters of OWN160 and TW160.

Parameters	OWN160	TW160
Design Range (nm)	2875	
Gross Takeoff Weight (lb)	141,868	146,251
Wingspan (ft)	112.2	114.0
Aspect Ratio	11.0	
Main Gear Type	2 wheel, 737-like	
Main Gear Length (in)	87.0	125.0
Nose Gear Length (in)	61.0	88.0
Cruise Mach	0.78	
Engine Model	Geared Turbofan	
Fan Diameter (in)	84.0	
Nacelle Max Diameter (in)	101.6	
Bypass ratio at SLS (Sea Level Static)	27.4	
Fan pressure ratio at SLS	1.18	
Thrust (lbf, single engine, at SLS)	21,600	21,500

The N+2 engine models were developed after incorporating the results of the ITD (Integrated Technology Demonstrator) studies [6, 11]. The OWN160 and TW160 feature the same small geared turbofan engine, details of which are shown in Table 2. Parameters are given for the top of climb (TOC) and sea level static (SLS) conditions. The thrust generated by these engines was less than current aircraft in this size class, due to the N+2 assumptions that the airframe would be lighter and more efficient than current aircraft.

Table 2 N+2 Engine modeling parameters.

Flight Condition	TOC	SLS
Architecture	Geared	
Mach, Altitude (kft)	0.8, 35.0	0.0,0.0
Net Thrust (lb)	4300	21550
Specific Fuel Consumption (lbm/(h·lbf))	0.4834	0.1914
Overall Pressure Ratio	35.00	24.85
Bypass Ratio	23.45	27.40
Fan Pressure Ratio	1.30	1.18

Seven ITDs were included in both vehicle designs. These concepts were developed and tested in ERA, with the most successful concepts being included in final aircraft models [6]. The following ITDs impacted the aircraft system level noise modeling of the OWN160, either directly or indirectly:

- ITD 12A+ Active Flow Control (AFC) Enhanced Vertical Tail plus Advanced Wing Flight Experiment with Insect Accretion Mitigation (IAM) and Natural Laminar Flow (NLF) features
- ITD 21A Damage Arresting Composites Demonstration
- ITD 21C Adaptive Compliant Trailing Edge (ACTE) Flight Experiment
- ITD 30A Highly Loaded Front Block Compressor
- ITD 35A Second Generation Ultra-High Bypass (UHB) Propulsor Integration
- ITD 40 Low NOx Fuel Flexible Combustor Integration
- ITD 50A Flap Edge and Landing Gear Noise Reduction

ITD 50A developed noise reduction technology for main landing gear and flap side edge airframe components. The flap side edge featured a porous side edge treatment to reduce noise by altering local steady and fluctuating pressure fields. A partial main landing gear fairing covered several structural elements to reduce turbulence and includes porous areas to provide flow through the fairing along edge serrations to minimize coherent shedding from the fairing sides. ITD 35A matured the soft vane technology, which is an acoustic treatment integrated into the stator vane of the fan bypass duct. Other N+2 noise reduction technologies included in the noise modeling were the multiple degree of freedom acoustic liner and interstage liner. Each technology had been validated experimentally in a representative environment at the time of study [6], making them feasible for inclusion in these aircraft models.

Both vehicles included high-lift systems with a Krueger flap leading edge device to enable natural laminar flow over the wing at cruise. The OWN160 and TW160 also include single element flap trailing edge devices to reduce discontinuities between flap elements. Flight-condition-specific parameters for the high-lift system (e.g., flap deflection angles, etc.) are used for the noise prediction. The OWN160 and TW160 include two-wheel 737-like main landing gear, with the primary difference being the main strut length.

Flight path plays a major role in noise predictions — Mach number and angle of attack influence airframe source noise levels, and altitude changes the acoustic propagation distance to observers. As shown in Fig. 4, the OWN160 has a higher altitude takeoff flight profile than the TW160, which is due to several factors. The two vehicles have different geometries, and the OWN160 weighs less than the TW160 due in part to the smaller landing gear and absence of pylons. However, this altitude difference (approximately 200 feet at 28000 feet from brake release) provides only a small benefit to certification noise.

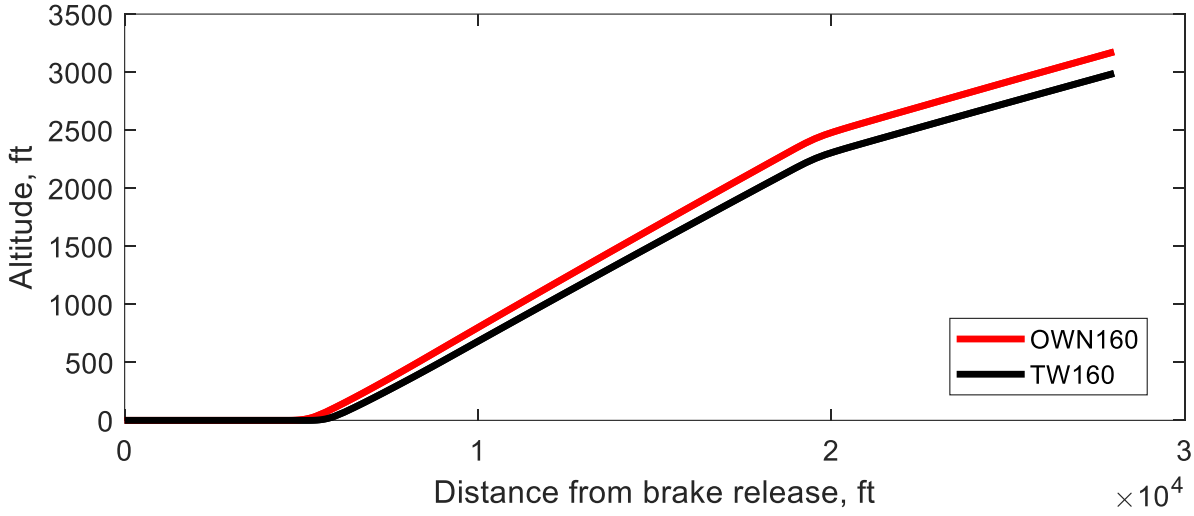

Fig. 4 OWN160 and TW160 takeoff flight profiles.

Table 3 provides further detail about the vehicle flight paths at the certification points for the OWN160 and TW160. The OWN160 moves slower at lateral and flyover points, which could lead to reduced airframe noise but will not reduce engine noise emission. Slower speeds can also negatively impact the EPNL (effective perceived noise level) calculation with longer integration times.

Table 3 Flight path parameters of the OWN160 and TW160.

		Climb Angle (°)	Angle of Attack (°)	Thrust Fraction	Speed (knots)
Approach	OWN160	-3.0	6.1	0.18	150
	TW160	-3.0	6.1	0.19	149
Lateral	OWN160	10.0	7.5	1.00	161
	TW160	9.5	6.6	1.00	167
Flyover	OWN160	5.0	8.5	0.68	161
	TW160	4.9	7.3	0.68	167

III. Noise Prediction Process

The FAA defines noise limits following the guidelines in 14 CFR Part 36 [12]. Noise metrics must be met for approach, full power departure (lateral), and departure engine cutback (flyover) locations, which correspond to the stages of flight with the greatest noise impact on communities surrounding airports, as shown in Fig. 5. The limits are defined in EPNdB, which is calculated by integrating the time history of the tone corrected perceived noise level (PNLT) for each observer position. This process considers duration, amplitude, spectral character, and human annoyance factors. The maximum allowable EPNL at each certification point is defined by the aircraft weight and number of engines. An additional constraint is levied on the cumulative (i.e., algebraic sum of the three certification levels) level. For Stage 5, the cumulative margin to the sum of the individual maximum allowable limits must be a minimum of 17 EPNdB. As noted in Section I, the NASA goals are relative to the Stage 5 margin, rather than the margin to the maximum limits. These same metrics are used to evaluate future aircraft and noise reduction concepts to quantify their value on a system level using accepted standards.

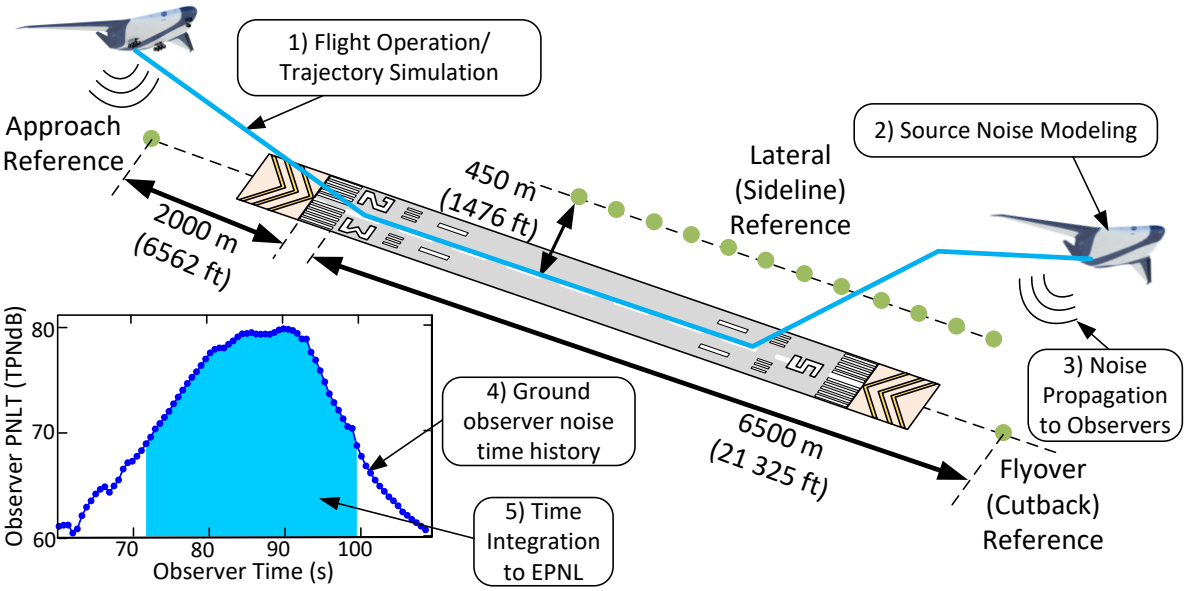

Fig. 5 Noise certification points with prediction methodology.

The internal research version of the NASA Aircraft NOise Prediction Program (ANOPP-Research) is used for this noise prediction. ANOPP2 serves as a framework for the ANOPP–Research version code, which features several models not present in the publicly released ANOPP. The methodology adopted over the last several years during the ERA project places heavy emphasis on the use of relevant experimental data and physics-based methods, which are compatible with complex, unconventional aircraft. This is reflected in the addition of the GUO-LG [13], GUO-FLAP, and GUO-LE [14] modules. The current publicly available version of ANOPP features mainly empirical or semiempirical relations, which are more suited to conventional aircraft design philosophies. The progression and development of the noise prediction process during the ERA project is detailed in Thomas et al. [2, 15]. An additional key advancement in recent years has been the ability to directly predict propulsion airframe aeroacoustic (PAA) effects, including engine noise shielding and reflection effects of the airframe, using experimental databases and

unique data processing tools. Figure 6 shows the overall noise prediction process and methods. A noise prediction starts with inputs – experimental data inputs for the prediction of both PAA effects and individual noise sources and design inputs that provide vehicle geometry and detailed aircraft performance data. Within ANOPP-Research, each individual noise source is modeled and appropriate noise reduction technology assumptions are applied. Then, PAA effects are applied, and the noise sources are summed to create a noise hemisphere. The flight path and atmosphere definitions are used to propagate the noise from this hemisphere to the ground at each certification point to obtain one-third octave band spectra and EPNL results.

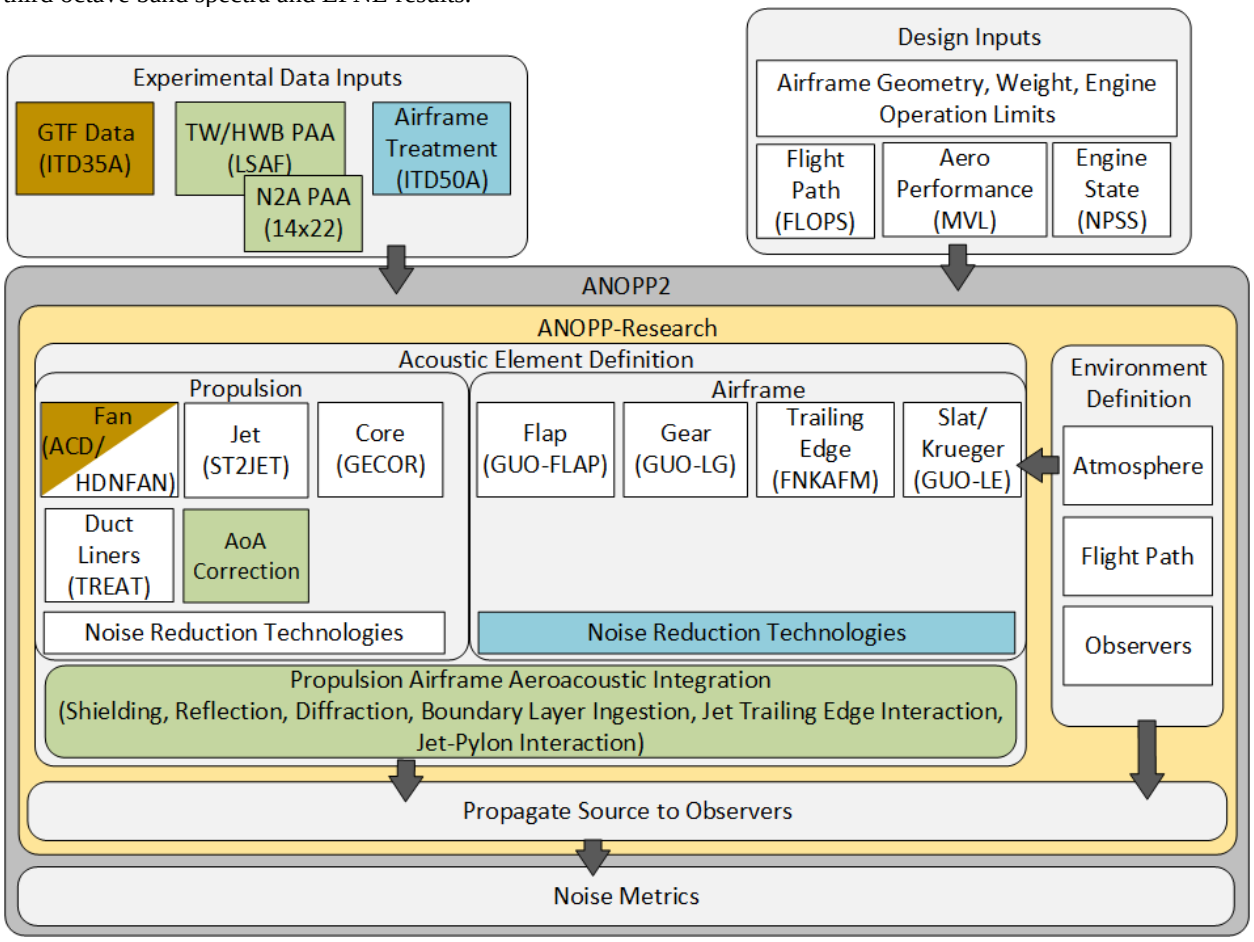

Fig. 6 Overview of the prediction process using ANOPP-Research in the current study [16].

In the ERA acoustic evaluation, the TW160 had a cumulative margin to Stage 4 noise requirements of 30.1 EPNdB, or 31.4 EPNdB with the three additional ITDNR technologies included. For the OWN160, these values were 40.2 and 41.1 EPNdB, respectively. Since the time of these analyses, multiple improvements have been made to ANOPP-Research and the system noise assessment process, including the addition of the GUO models for flap and leading edge noise [13, 14]. The implementation of SAE ARP 866A for atmospheric absorption has been corrected. The liner attenuation model has been modified to use a Strouhal number criterion to determine the lower frequency limit, rather than a fixed one-third octave band frequency. Also, outer stream mixing noise and plug separation noise are now included in the jet noise prediction, following comparisons with experimental data showing that the inclusion of these effects leads to more accurate results [16].

IV. Modeling PAA Effects

PAA effects include any acoustic or flow interaction effects due to integration of the engine and airframe that create new sources or alter the acoustic sources of the aircraft. They can play a large role, favorable or adverse, in system noise results as seen in the ERA studies where PAA effects changed the EPNL by up to 7 EPNdB [2, 17]. For the OWN configuration, the primary PAA effects are the engine noise shielding and the jet flow interaction with the

wing. The latter includes jet scrubbing and Jet-TE interaction. Jet scrubbing occurs as jet exhaust flows past an adjacent surface which creates turbulence-induced noise but does not include any edge effects. For an OWN configuration, jet scrubbing occurs on the top surface of the wing and is not a significant source for observers on the ground. Jet-TE interaction noise occurs as the jet exhaust passes over the trailing edge of the wing and the pressure fluctuations associated with turbulence traversing past the trailing edge cause scattering noise. Head and Fischer [18] first documented a Jet-TE noise increase at low frequencies in 1976, where they observed an additional noise source that had a downstream dipole directivity. However, it is reasonable to consider the Jet-TE interaction noise as an enhancement of trailing edge self-noise, with the edge scattering the hydrodynamic pressure fluctuations within the jet flow, rather than those within a turbulent boundary layer. This would suggest that the source would have a half-dipole behavior with stronger radiation in the forward direction [19]. More recent studies have investigated this source further and characterized the low frequency noise increase along with the factors influencing it, such as position and jet flow condition [20,21]. Since much of the aft-radiated engine and jet noise will be shielded by the wing, Jet-TE interaction noise is a potentially important source for OWN configurations. The TW160 engine is mounted on a pylon and placed further away from the wing, so Jet-TE interaction noise is not expected for that configuration. To determine the impact of this effect, experimental data are used to create a noise model for Jet-TE interaction.

During the ERA project, NASA collaborated with Boeing and performed a series of PAA interaction experiments in the Boeing Low Speed Aeroacoustics Facility (LSAF) [22-24]. The previously unpublished results from one of this series, a 2009 experiment involving a 4.7% scale Boeing 777 airframe model and a 4.7% scale GE90-115B jet noise simulator with heated flow, are used to model Jet-TE effects for OWN-like configurations, as shown in Fig. 7. In the test, the airframe was mounted on a traverse and could be moved to various positions relative to the jet noise simulator, including multiple over- and under-wing positions. Forty-one microphones were used to record data. Their positions are denoted by polar and azimuthal angles, where the polar angle is represented by θ with 0° in the direction of flight and the azimuthal angle is represented by Φ with 0° directly under the flight path. One row of microphones was located directly 'beneath' the airframe at 0° azimuth, and the other two rows were located at 30° and 60° relative to this position.

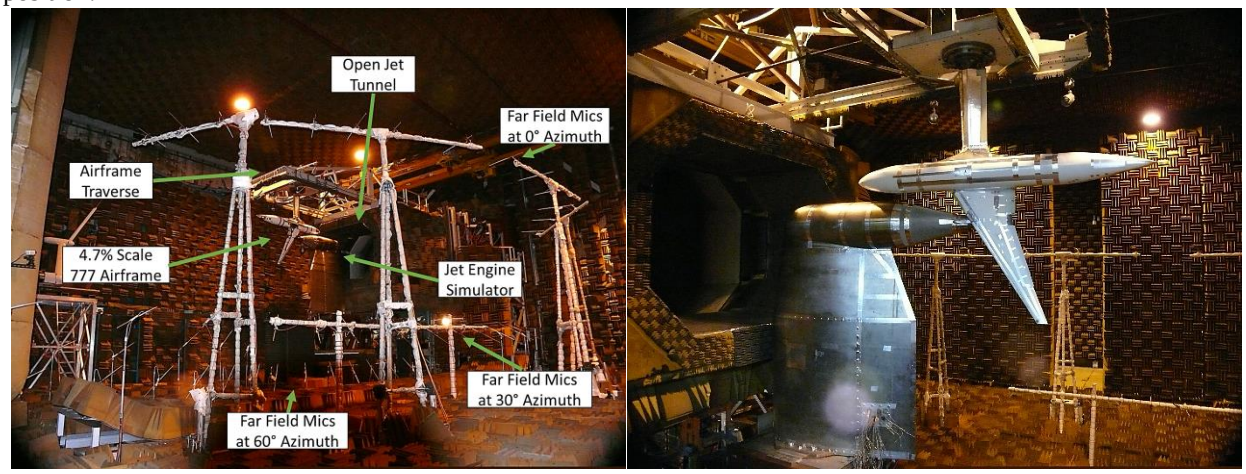

Fig. 7 NASA/Boeing LSAF PAA experimental setup [photo credit: The Boeing Company].

Multiple over-wing aircraft positions were investigated during this study, which were defined relative to a nominal 777 engine position, as shown in Fig. 8. These ranged from 0 to 1.2 nozzle diameters forward of the nominal position and 1.2 to 1.44 nozzle diameters above the nominal position. The relative airframe/engine positions were limited by the size of the engine model hardware. Multiple engine conditions were modeled during this study, with primary (core) nozzle pressure ratios from 1.3 to 1.7, primary temperature ratios from 2.6 to 3.1, secondary (bypass) nozzle pressure ratios from 1.5 to 1.8, and secondary temperature ratios from 1.1 to 1.2. A 1.3 primary pressure ratio and 1.5 secondary pressure ratio condition were chosen for this noise model to represent the N+2 engine conditions of the OWN160.

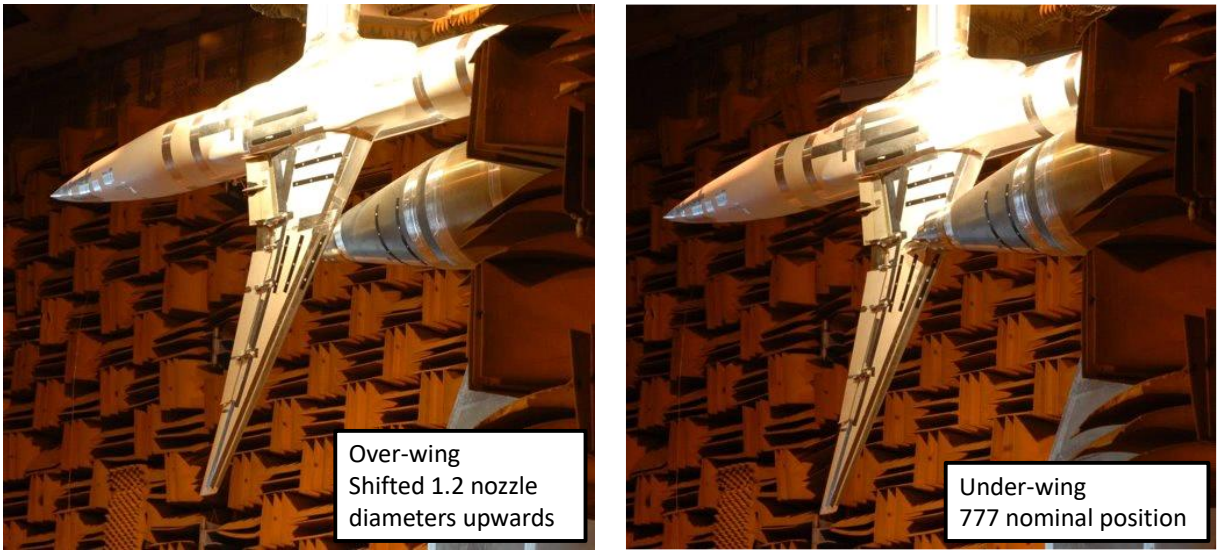

Fig. 8 Over- and under-wing positions for NASA/Boeing LSAF PAA test [photo credit: The Boeing Company].

Figure 9 shows low frequency acoustic results for engine model positions shifted 1.2 and 1.44 diameters upward from the nominal 777 position, as well as the isolated engine noise model. A noise increase at low frequencies is observed for the aircraft position with the engine model closest to the airframe. This increase is caused by interaction between the jet and the trailing edge of the airframe. Figure 9 shows the frequency spectrum results for a microphone position at an azimuthal angle of 0° and a polar angle of 60°, directly beneath and forward of the airframe. This noise increase is not observed for the more upstream or further upward engine positions when the trailing edge is not within the jet exhaust plume. At higher frequencies, the noise is lower than the isolated engine case due to shielding. Noise shielding also occurs at low frequencies, but the Jet-TE interactions at low frequencies involve very energetic vortices such that the noise increase overwhelms the shielding effects. The most significant noise increases are seen at forward emission angles, as shown in Fig. 9. This forward radiation is consistent with other studies, which describe the source as a half-dipole with stronger radiation in the forward direction [19, 25].

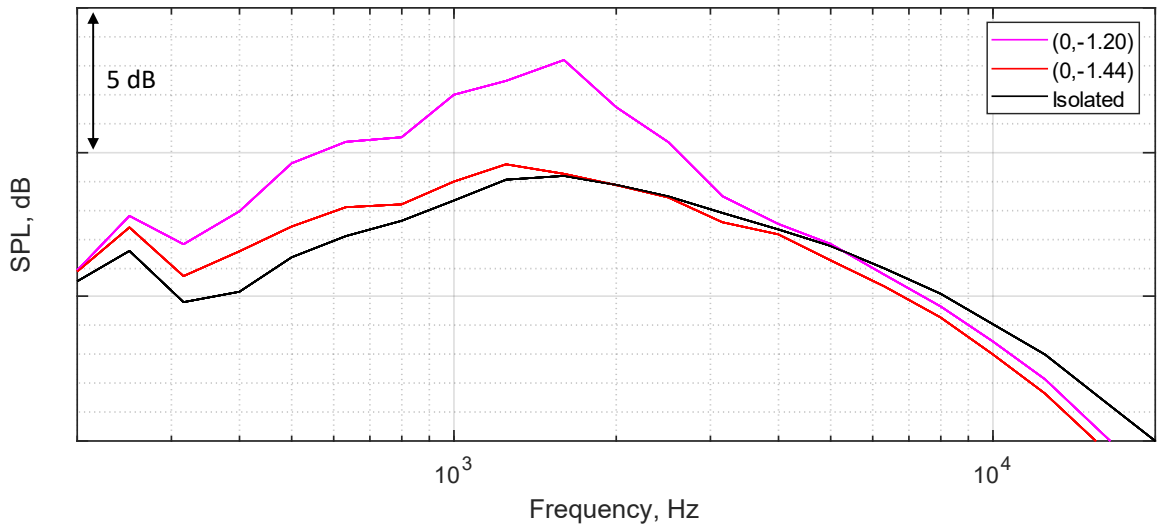

Fig. 9 Jet-TE interaction noise observed in LSAF PAA experiments, model-scale, (Φ = 0°, θ = 60°).

The difference between the closest OWN position (shifted 1.2 nozzle diameters) and the isolated engine case is calculated for all microphone positions and linearly interpolated to obtain the suppression maps shown in Fig. 10. For this figure, only the noise increase due to Jet-TE interaction is being considered, so all negative Δ SPL (sound pressure level) values (i.e., where shielding is present) are set to zero. Shielding models are discussed later in this section.

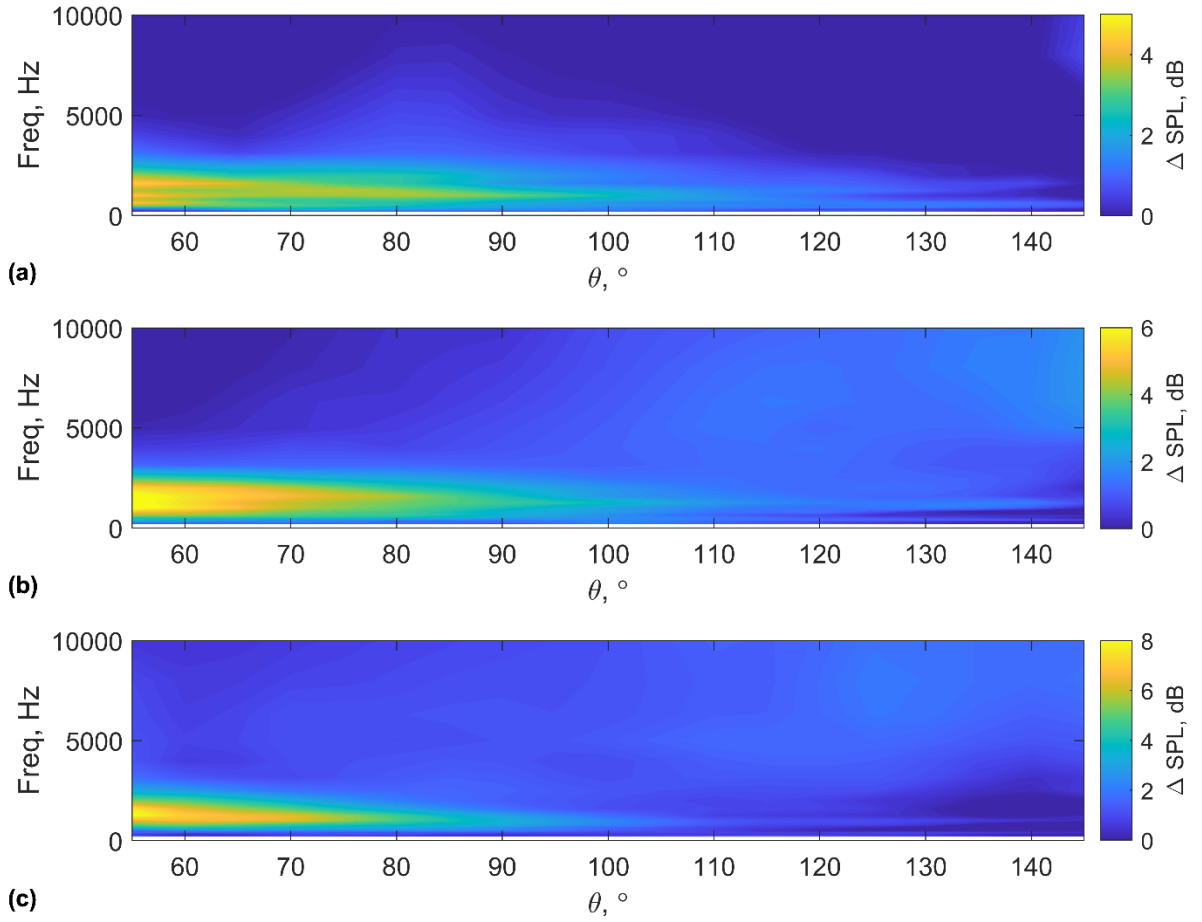

Fig. 10 ΔdB noise increase between isolated and installed OWN position at model-scale for (a) Φ = 0°, (b) Φ = 30°, and (c) Φ = 60°.

The results from these model-scale (*MS*) experiments are scaled to full-scale (*FS*) before being incorporated into the system noise assessment. Frequency (*f*) scaling is done by equivalent Strouhal number, based on nozzle diameter (*D*) and bypass jet flow velocity (*U*) as shown in Eqs. (1-2). Equation (3) shows the equivalent frequency relationship between model and full-scale. The bypass jet flow velocity is used for scaling, in lieu of the core velocity, because the primary interaction will occur with the bypass flow.

$$Strohal\ Number = \frac{diameter * frequency}{velocity} \tag{1}$$

$$St = \frac{f_{MS} D_{j,MS}}{U_{j,MS}} = \frac{f_{FS} D_{j,FS}}{U_{j,FS}} \tag{2}$$

$$f_{FS} = f_{MS} * \frac{D_{j,MS}}{D_{j,FS}} * \frac{U_{j,FS}}{U_{j,MS}} \tag{3}$$

Amplitude scaling is done based on the expected Mach (M) number relationships of each source. For the one-third octave band sound pressure levels, jet mixing noise scales with M^8 for the jet flow and the Jet-TE interaction source scales with M^5. Because of the high bypass ratios of the N+2 engine models, the bypass flow dominates the total jet velocity, and the bypass Mach number is used for the amplitude scaling in all cases. The scaling rules for the isolated sources are shown in Eqs. (4–7). Due to the different Mach number dependencies, the relative levels between the jet mixing noise and the Jet-TE source vary depending on the jet Mach number. Equation (6) is subtracted from Eq. (7) to get the relationship shown in Eq. (8), which relates the SPL difference at model-scale to the SPL difference at full-scale with the additional scale factor from the Mach number relationship.

$$SPL_{iso} \sim M^8 \tag{4}$$

$$SPL_{inst} \sim M^5 \tag{5}$$

$$SPL_{iso,FS} = SPL_{iso,MS} + 80\log_{10}\left(\frac{M_{FS}}{M_{MS}}\right) \tag{6}$$

$$SPL_{inst,FS} = SPL_{inst,MS} + 50\log_{10}\left(\frac{M_{FS}}{M_{MS}}\right) \tag{7}$$

$$\Delta SPL_{FS} = \Delta SPL_{MS} - 30\log_{10}\left(\frac{M_{FS}}{M_{MS}}\right) \tag{8}$$

A threshold of 2 dB is used, so the noise increase from the Mach number relationship is only applied at frequencies where the Jet-TE interaction source is significantly dominant (by at least 2 dB) over the jet mixing noise and reflections. Reflection from the fuselage causes a significant area of noise increase in the aft direction at high frequencies, as shown in Fig. 10. More reflection is observed at higher azimuthal positions (comparing upper right corner of each contour plot in Fig. 10), which aligns with the reflection path for the aft radiated engine noise off the fuselage, as shown in Fig. 8. The 2 dB threshold factor rejects the observed regions of reflection so that the amplification factor is only applied to the regions where Jet-TE interaction is expected, in the forward directions at low frequencies. The ΔSPL_{FS} of Eq. (8) is applied to the jet noise source in ANOPP-Research, as described in Section III.

Fan shielding is incorporated using a similar process, which also utilizes a dataset from the NASA/Boeing PAA experiments with the 4.7% scale 777 airframe model and a broadband noise simulator in a nacelle to represent broadband fan noise. The shielding models and experimental datasets are identical to those used in the previous ERA studies. Frequency scaling for the shielding models is done in relation to the experimental and full-scale geometries, and no amplitude scaling is performed. Similarly, jet shielding is accounted for with a dataset using the 777 airframe and a nozzle model more relevant to the ultra-high bypass ratio N+2 engine models. Future studies may include Jet-TE interaction and shielding from the same dataset to better understand how these two acoustic mechanisms may impact each other.

V. Results

In this study, the ERA system noise analysis from 2016 is updated with improved noise models. A Jet-TE noise model is created based on experimental data, and the impact of this model on system-level noise is evaluated. Results from the updated analysis are compared with an updated TW160 prediction. The effect of Jet-TE interaction is applied to the jet noise source and is shown to cause a low frequency noise increase, especially at the forward positions.

A) Approach

The PNLT breakdown of the OWN160 at the approach certification point is shown in Fig. 12 with and without the Jet-TE interaction effect applied. As noted in Fig. 12, the fan, core, and jet noise sources have additional PAA effects applied, such as shielding and reflection. Despite the shielding effect of the wing, fan noise is dominant for the OWN160 with and without Jet-TE interaction. Krueger and flap noise also contribute significantly to the total PNLT near the peak. Landing gear, core, and trailing edge noise levels are all significantly lower and contribute only minimally to the total levels. Although the Jet-TE interaction effect significantly increases the jet noise, particularly

at earlier reception times when the jet-interaction noise is emitted in the forward direction, the low power setting of the engine (i.e., thrust fraction of 0.18) means that the jet noise is not a significant contributor to the total noise in either case.

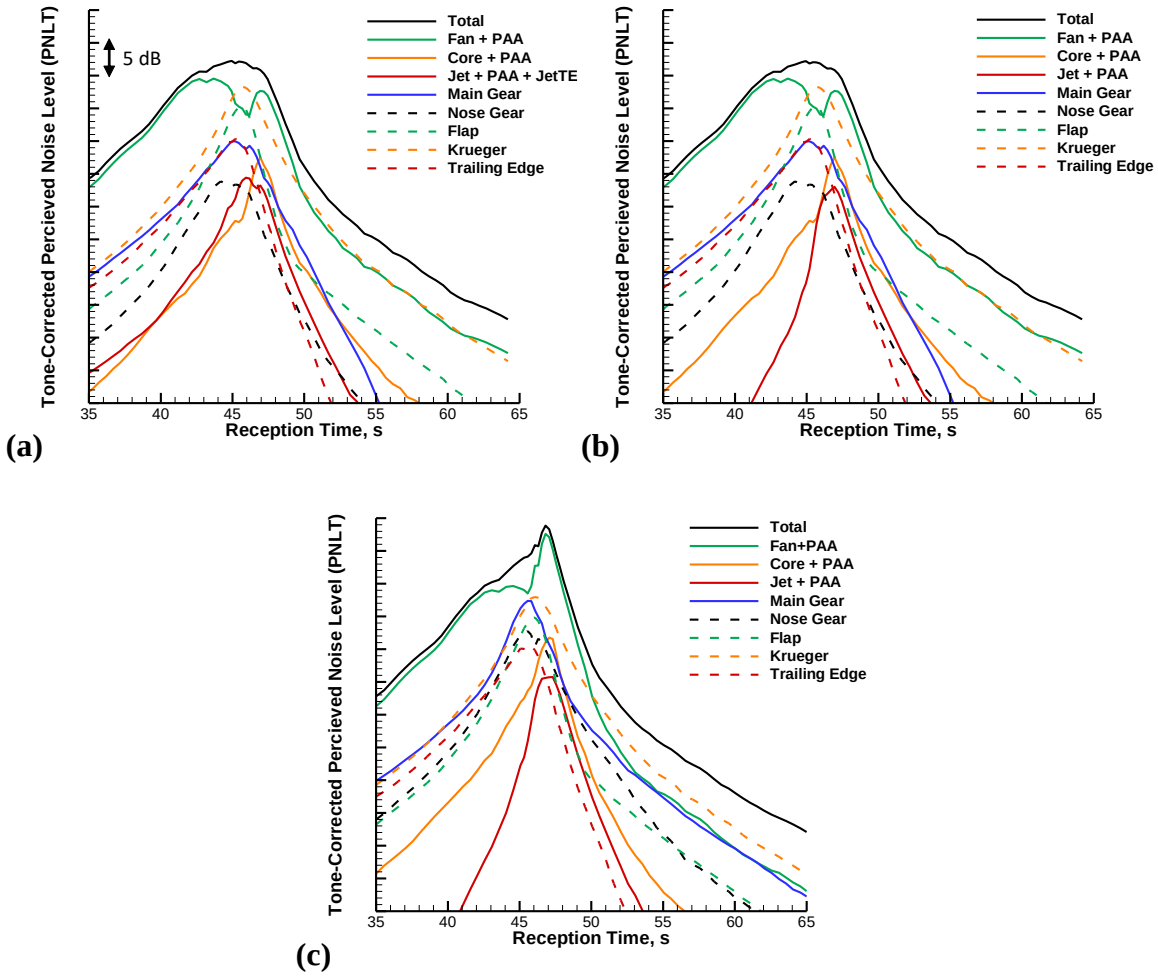

Fig. 12 PNLT curves of noise received by approach observer (thrust fraction = 0.18) for the (a) OWN160 with Jet-TE interaction, (b) OWN160 without Jet-TE interaction, and (c) TW160.

Figure 12 also shows a comparison between the best, most complete prediction of the OWN160 (i.e., including the Jet-TE interaction effect) and the conventional TW160 configuration. The source ranking of the OWN160 is different than its conventional counterpart. TW160 noise is largely dominated by fan noise due to the lack of shielding and added reflection of aft-radiated fan noise. Despite this, the Krueger and main gear noise also contribute significantly to the total PNLT, particularly before the peak where those sources radiate significant noise to forward angles. Comparison with the OWN160 shows that the shorter landing gear are significantly quieter, confirming that the shorter gear enabled by the OWN160 are an important feature to retain in order to realize the full acoustic potential of this configuration. Jet noise extends more forward for the OWN160 when compared to the TW160 due to the Jet-TE interaction effect, but is not a significant noise source for the approach condition.

B) Flyover

A similar comparison between OWN160 configurations (i.e., with and without the Jet-TE interaction effect) is given in Fig. 13 for the flyover certification point. Due to the higher thrust at this condition, a thrust fraction of 0.68, jet noise is a more significant contributor to the total aircraft noise, such that the Jet-TE interaction effect now directly alters the source ranking. Without this interaction effect, fan noise, especially in the aft quadrant, is highly dominant,

followed by core noise, and Krueger noise contributes more in the forward quadrant. With the interaction effect applied, jet noise exceeds Krueger noise in the forward quadrant and is the leading contributor to total PNLT just prior to the peak. Other airframe sources (i.e., flap and trailing edge) are negligible contributors to the total aircraft PNLT.

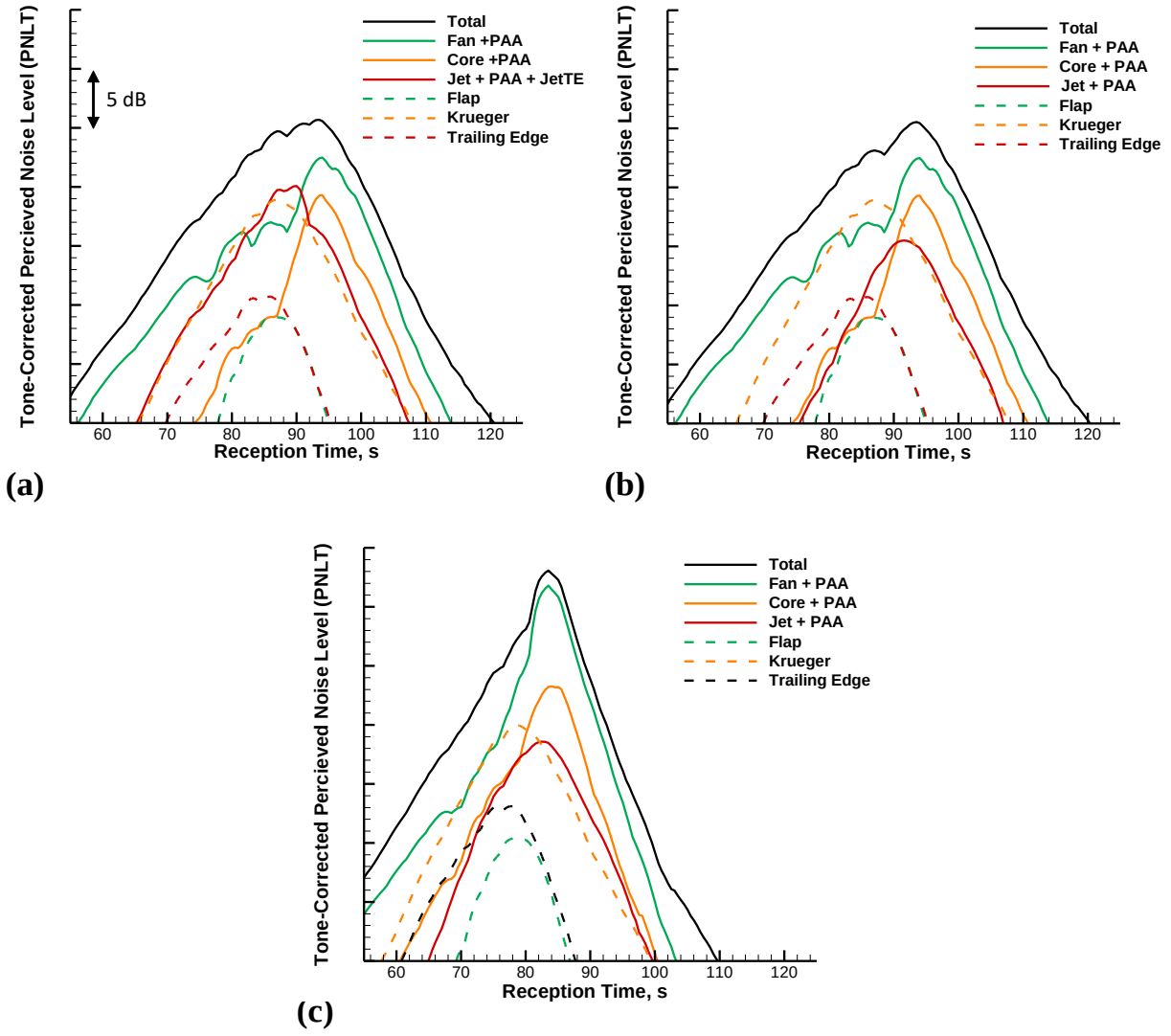

Fig. 13 PNLT curves of noise received by flyover observer (thrust fraction = 0.78) for the (a) OWN160 with Jet-TE interaction, (b) OWN160 without Jet-TE interaction, and (c) TW160.

Considering again a comparison between the OWN160 and TW160 during flyover, fan noise is still dominant for both configurations, but other sources on the TW160 are largely irrelevant due to the high levels of fan noise emitted in the aft direction due to reflections. Core noise is the next leading source for the TW160 since it is also influenced by reflections from the wing. With Jet-TE interaction, jet noise is the second highest contributor for the OWN160, while it is the fourth highest contributor for the TW160.

C) Lateral

Finally, considering the same comparisons at the lateral certification point, thrust is maximum (i.e., thrust fraction of 1.0), and jet noise is most significant at this condition for the total system noise, as shown in Fig. 14. The total noise is dominated by noise from the fan and jet, although the Jet-TE interaction effect increases the peak jet noise to within 2 dB of the fan noise. Jet-TE interaction noise affects the forward direction, where fan noise tends to be less dominant.

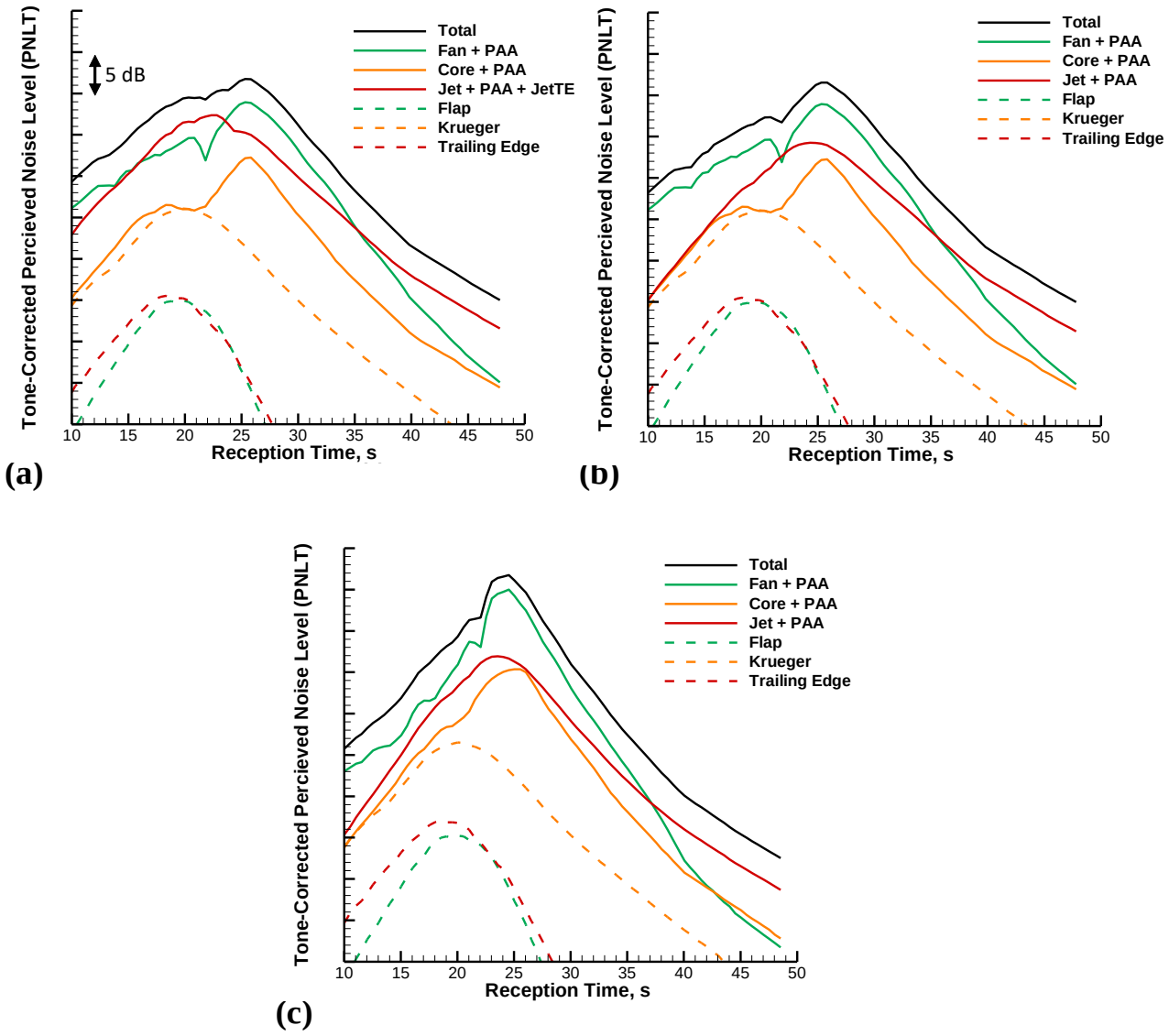

Fig. 14 PNLT curves of noise received by lateral observer (thrust fraction = 1.0) for the (a) OWN160 with Jet-TE interaction, (b) OWN160 without Jet-TE interaction, and (c) TW160.

While fan and jet noise are similar in magnitude for the OWN160, the TW160 noise is more dominated by fan noise at all but the aftmost angles, especially in the forward direction. Jet noise is a second contributor to overall levels, followed by core noise.

D) Cumulative Results

To provide a high-level overview of the different configurations and comparison with the TW160, Fig. 15 presents PNLT time histories of total and jet noise for all OWN160 configurations and the TW160. The TW160 has the highest total PNLT at each certification point, followed by the OWN160 with Jet-TE interaction, the OWN160 without Jet-TE interaction, then the ERA OWN160. Jet noise is significantly higher in the updated OWN160 prediction than the ERA OWN160 prediction. The ERA noise models did not include outer stream mixing noise in the jet noise prediction, which significantly increases noise, especially at the approach certification point. Nonetheless, at the approach point, the jet noise increase is shrouded by other sources and does not affect the overall PNLT as much as at the lateral and flyover positions. In general, jet noise is a larger contributor to total noise for the OWN configurations than the TW configuration, which is more dominated by fan noise.

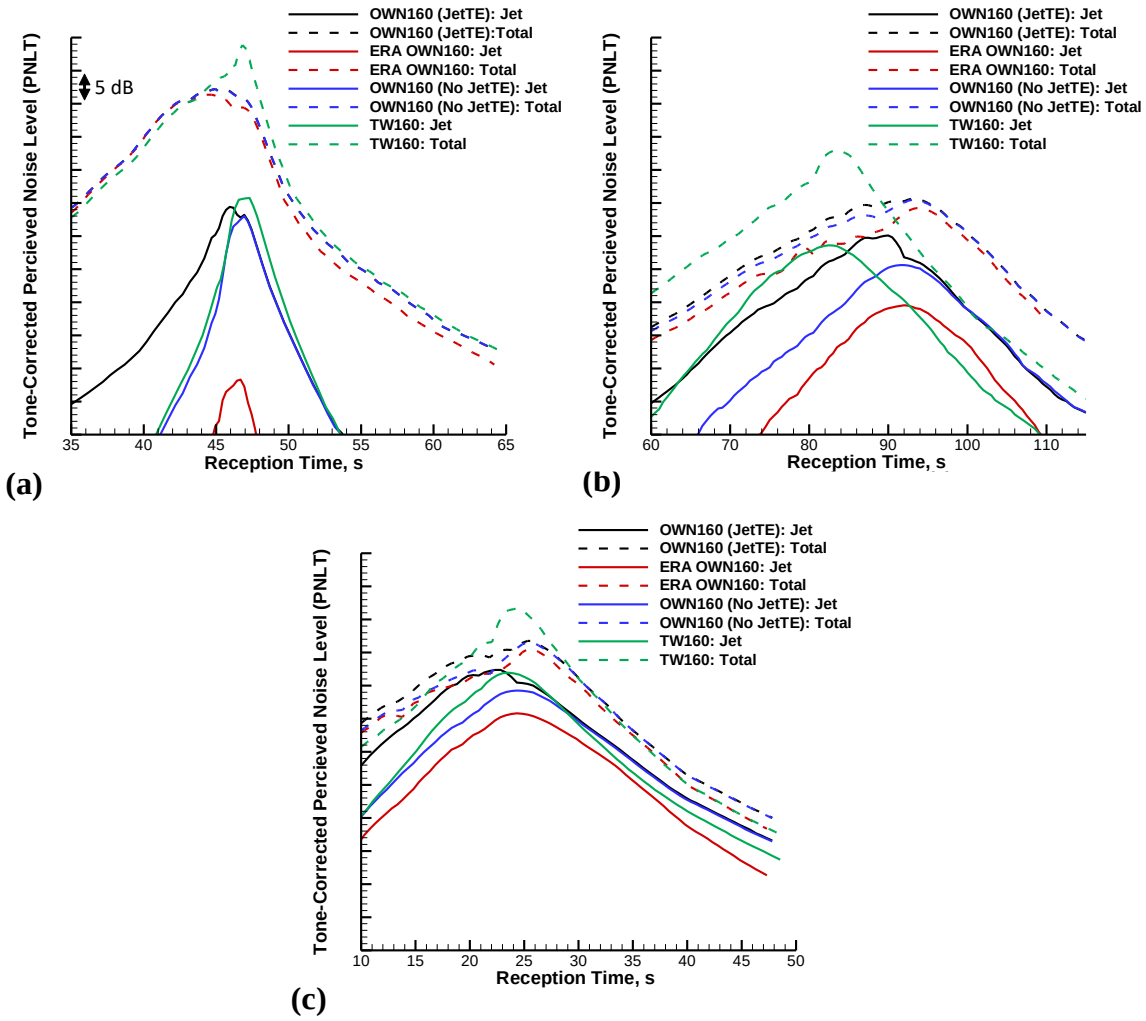

Fig. 15 PNLT curves of jet and total noise received by observer for OWN160, OWN160 with Jet-TE interaction, ERA OWN160, and TW160 at (a) approach, (b) flyover, and (c) lateral positions.

These trends are also reflected in the EPNL values, shown in Table 4. Results are presented relative to Stage 3 (reference limits) and Stage 5 noise requirements, where higher margins indicate a quieter aircraft. The ERA OWN160 is 3.0 EPNdB cumulative quieter than the updated OWN160 prediction without Jet-TE interaction and 4.6 dB quieter than the updated OWN160 with Jet-TE interaction. Most of the difference is in the lateral and flyover certification points. With Jet-TE interaction included, the OWN160 is 7.7 EPNdB quieter than the updated TW160 configuration, with significant benefit at all three certification points.

Table 4 EPNdB values for OWN160 with Jet-TE interaction, OWN160, ERA OWN160, and TW160.

Configuration	Approach	Lateral	Flyover	Cumulative	Cumulative Margin relative to Stage 5	Cumulative Margin relative to Limits
OWN160 with Jet-TE	84.8	82.3	73.3	240.5	29.5	46.5
OWN160	84.8	81.5	72.6	238.9	31.1	48.1
ERA OWN160	84.2	80.7	71.0	235.9	34.1	51.1
TW160	87.1	84.1	77.0	248.2	21.8	38.8
Limits at each certification point	99.9	90.4	96.1	-	-	-

The noise assessment improvements increase the overall predicted noise levels of the OWN160, and the inclusion of Jet-TE interaction source also increases the jet and total noise. Despite these increases, the OWN160 is still a competitive concept when compared to a conventional vehicle configuration, with cumulative noise 7.7 EPNdB quieter than the TW160.

VI. Concluding Remarks

The NASA OWN160 model is an unconventional aircraft concept that has potential benefits for fuel efficiency, emissions, and noise. A comprehensive noise assessment using ANOPP-Research was performed for this design. Jet-TE interaction was considered, and an experimental model was created using data from a 2009 NASA/Boeing PAA experiment in the LSAF facility. This model was applied to the system noise prediction of the OWN160, and the Jet-TE interaction effect increased the cumulative noise levels by 1.6 EPNdB. This effect is significant and further illustrates that all relevant PAA effects should be considered in future vehicle analyses for higher fidelity and more accurate system noise. The results were compared to an equivalent conventional aircraft model, the TW160. With the jet-trailing-edge interaction source, the OWN160 still performs favorably when compared to the conventional configuration, with a cumulative reduction of 7.7 EPNdB. This reduction is due, in large part, to favorable PAA effects such as shielding. When compared to the prior ERA noise prediction, the updated noise models predict a 3.0 dB noise increase, consistent with other aircraft model updates. The updated acoustic models are more physics-based and comprehensive than the older models and provide a more accurate representation of the total aircraft noise.

Future work will include creating a noise model for Jet-TE and shielding from the same experimental data set to better understand how these two effects interact with one another. Also, the Jet-TE noise model will be developed further to be applicable to more aircraft configurations and should be considered in future unconventional vehicle noise predictions. Further comprehensive analysis is required to enable the over-wing-nacelle configuration for future aircraft.

Acknowledgments

The authors thank the Advanced Air Transport Technology Project for their support. The authors also acknowledge the additional members of the PAA and Aircraft System Noise Team of the Aeroacoustics Branch at NASA Langley Research Center for assisting with this study. The engine definitions were provided by the Propulsion Systems Analysis Branch at NASA Glenn Research Center. The airframe and flight path definitions were provided by the Aeronautics Systems Analysis Branch at NASA Langley Research Center. Artist renderings of the aircraft and engines were provided by Analytical Mechanics Associates studios.

References

[1] National Aeronautics and Space Administration, “NASA Aeronautics: Strategic Implementation Plan,” 2019, pp. 37–43.

[2] Thomas, R. H., Burley, C. L., and Nickol, C. L., "Assessment of the Noise Reduction Potential of Advanced Subsonic Transport Concepts for NASA Environmentally Responsible Aviation Project," in *54th AIAA Aerospace Sciences Meeting*, 2016. https://doi.org/10.2514/6.2016-0863

[3] Kinney, D., Hahn, A., and Gelhausen, P., "Aerodynamic Investigations of an Advanced Over-the-Wing Nacelle Transport Aircraft Configuration," *Journal of Aircraft*, vol. 46, January 2009. https://doi.org/10.2514/6.2007-670

[4] Kinney, D., Hahn, A., and Gelhausen, P., "Comparison of low and high nacelle subsonic transport configurations," *15th Applied Aerodynamics Conference*, 1997. https://doi.org/10.2514/6.1997-2318

[5] Kinney, D., and Hahn, H., US Patent for a “Aircraft Wing for Over-The-Wing Mounting of Engine Nacelle,” U.S. Patent No. 7,883,052, issued February 8, 2011.

[6] Nickol, C. L., and Haller, W. J., "Assessment of the Performance Potential of Advanced Subsonic Transport Concepts for NASA's Environmentally Responsible Aviation Project," 2016. https://doi.org/10.2514/6.2016-1030

[7] Lan, C.E., and Campbell, J.F., "Theoretical Aerodynamics of Upper-Surface-Blowing Jet-Wing Interaction," NASA TN D-7936, 1975.

[8] McCullers, L. A., "Aircraft Configuration Optimization Including Optimized Flight Profiles," *Proceedings of the Symposium on Recent Experiences in Multidisciplinary Analysis and Optimization*, NASA CP-2327, 1984.

[9] Lytle, J. K., "The Numerical Propulsion System Simulation: An Overview," NASA TM-2000-209915, 2000.

[10] Tong, M.T., Naylor, B.A., "An Object-Oriented Computer Code for Aircraft Engine Weight Estimation," *Gas Turbine Technical Congress and Exposition*, 2008. https://doi.org/10.1115/gt2008-50062

[11] Van Zante, D.E., and Suder, K.L., "Environmentally Responsible Aviation: Propulsion Research to Enable Fuel Burn, Noise, and Emissions Reduction," International Symposium on Air Breathing Engines, 2015.

[12] *Noise Standards: Aircraft Type and Airworthiness Certification*, Code of Federal Regulations, Title 14, Chapter 1, Part 36, January 2021.

[13] Guo, Y., Burley, C. L., and Thomas, R. H., "Landing Gear Noise Prediction and Analysis for Tube-And-Wing and Hybrid-Wing-Body Aircraft," *54th AIAA Aerospace Sciences Meeting*, January 2016. https://doi.org/10.2514/6.2016-1273

[14] Guo, Y., Burley, C. L., and Thomas, R. H., "Modeling and Prediction of Krueger Device Noise," *22nd AIAA/CEAS Aeroacoustics Conference*, May 2016. https://doi.org/10.2514/6.2016-2957

[15] Thomas, R.H., Burley, C.L., and Guo, Y., "Progress of Aircraft System Noise Assessment with Uncertainty Quantification for the Environmentally Responsible Aviation Project," *22nd AIAA/CEAS Aeroacoustics Conference,* 2016. https://doi.org/10.2514/6.2016-3040

[16] June, J.C., Thomas, R.H., and Guo, Y., "System Noise Prediction Uncertainty Quantification for a Hybrid Wing-Body Transport Concept," *AIAA Journal,* Vol. 58, No. 3, March 2020. https://doi.org/10.2514/6.2018-3125

[17] June, J.C., Thomas, R.H., Guo, Y., and Clark, I.A., "Far Term Noise Reduction Technology Roadmap for a Large Twin-Aisle Tube-and-Wing Subsonic Transport," *25th AIAA/CEAS Aeroacoustics Conference,* 2019. https://doi.org/10.2514/6.2019-2428

[18] Head, R.W., and Fisher, M.J., "Jet/Surface Interaction Noise: - Analysis of Farfield Low Frequency Augmentation of Jet Noise due to the Presence of a Solid Shield," *3rd AIAA Aero-Acoustics Conference*, 1976. https://doi.org/10.2514/6.1976-502

[19] Ffowcs Williams, J.E., and Hall, L.H., "Aerodynamic Sound Generation by Turbulent Flow in the Vicinity of a Scattering Half Plane," *Journal of Fluid Mechanics,* vol. 40, part 4, 1970. https://doi.org/10.1017/s0022112070000368

[20] Brown, C., "Jet-Surface Interaction Test: Far-Field Noise Results," *ASME Turbo Expo 2012: Turbine Technical Conference and Exposition,* 2012. https://doi.org/10.1115/gt2012-69639

[21] Brown, C., "An Empirical Jet-Surface Interaction Noise Model with Temperature and Nozzle Aspect Ratio Effects," *AIAA Scitech,* 2015. https://doi.org/10.2514/6.2015-0229

[22] Czech, M.J., Thomas, R.H., and Elkoby, R., "Propulsion Airframe Aeroacoustic Integration Effects of a Hybrid Wing Body Aircraft Configuration," *International Journal of Aeroacoustics,* Vol. 11 (3+4), pp. 335-368, 2012. https://doi.org/10.2514/6.2010-3912

[23] Thomas, R.H., Czech, M.J., and Doty, M.J., "High Bypass Ratio Jet Noise Reduction and Installation Effects Including Shielding Effectiveness," *51st AIAA Aerospace Sciences Meeting including the New Horizons Forum and Aerospace Exposition,* 2013. https://doi.org/10.2514/6.2013-541

[24] Czech, M.J. and Thomas, R.H., "Open Rotor Aeroacoustic Installation Effects for Conventional and Unconventional Airframes," *19th AIAA/CEAS Aeroacoustics Conference,* 2013. https://doi.org/10.2514/6.2013-2185

[25] Cannell, P., and Ffowcs Williams, J.E., "Radiation from Line Vortex Filaments Exhausting from a Two-Dimensional Semi-Infinite Duct," *Journal of Fluid Mechanics,* vol. 58, part 1, 1973. https://doi.org/10.1017/s0022112073002132